ECG-Based Cardiac Disease Detection in Time-Frequency Domain using Grid Search Optimized Wavelet Transforms

Diwakar Diwakar^{1*}, Deepa Raj¹

¹Department of Computer Science, BBA University, Lucknow, India. *Corresponding author(s). E-mail(s): diwakarmsccs0@gmail.com

Abstract

Cardiovascular diseases(CVDs), including abnormal arrhythmias and congestive heart failure, are a leading cause of mortality worldwide, with electrocardiogram (ECG) signals serving as a critical diagnostic tool. This study introduces a novel approach for classifying diseases in ECG signals into three categories: normal sinus rhythm (NSR), abnormal arrhythmia (ARR), and congestive heart failure (CHF). The classification is based on a combination of features extracted from both the time domain (mean and standard deviation) and the frequency domain (power spectral density and spectral centroid) of the ECG signals. Additionally, energy values from selected frequency bands are utilized. To enhance the model's robustness, incorporate data augmentation techniques, including time-shifting and flipping of the signals. These augmented datasets are then employed with various classifiers, and an optimization process using grid search is applied to enhance the classification performance. This methodology presents a promising framework for automated ECG signal analysis, the results of the proposed work have been exceptionally promising, showcasing a remarkable specificity rate of 99.7% and achieving an accuracy level of 99.58%. These findings hold significant promise for advancing early detection methods and enhancing patient outcomes in the realm of CVDs.

Keywords: Electrocardiogram, Classification, time domain, frequency domain, wavelets

1 Introduction

Cardiac arrhythmias, characterized by abnormal heart rhythms, pose significant health risks and require an accurate and timely diagnosis for effective treatment. The automatic detection and classification of these conditions have become a focal point in biomedical research, with the aim of creating dependable, noninvasive diagnostic tools. Among the various diagnostic tools for cardiovascular diseases (CVDs), the electrocardiogram (ECG) is a fundamental, noninvasive technique that records the electrical activity of the heart over time. It provides crucial information about the heart's condition, including the presence of arrhythmias and signs of congestive heart failure. However, the manual interpretation of ECG signals can be time-consuming and requires a high level of expertise, leading to potential delays in diagnosis and treatment. The application of machine learning (ML) techniques to ECG signal analysis has been an area of active research in recent years. Several studies have demonstrated the potential of ML to enhance the accuracy and efficiency of ECG interpretation.

Sharma et al. [1] conducted a study on feature extraction in the context of heart-beat classification and arrhythmia detection. They utilized optimal orthogonal wavelet filters and obtained an accuracy rate of 98%.

Jing et al. [2] introduce an enhanced ResNet-18 model tailored for ECG heartbeat classification. They employ a slicing technique for data labelling, resulting in an impressive accuracy of 96.50%. An effective approach for detecting ventricular late potential based on an ECG signal and SVM classifier is proposed by Giorgio et al. [3], resulting in a positive predictively of 88.52%. Jha et al. [4] introduced a highly efficient method for classifying ECG beats, distinguishing between normal beats and seven types of arrhythmias. Their approach utilizes tunable Q-wavelet-based features and achieved an impressive average accuracy of 99.27%. Arumugam et al. [5] introduced a methodology centered around wavelets to identify and classify Arrhythmia, resulting in a positive predictively rate of 95.92%. Zhao et al. [6], introduced a Deep CNN approach that utilized a 24-layer CNN to extract features from ECG data through cross-size convolution kernels. The proposed method achieved an accuracy of 87.1% in ECG classification. Wang et al. [7] demonstrated a high accuracy of 98.74% in early arrhythmia detection by employing continuous wavelet transform (CWT) and convolutional neural networks (CNNs). A study conducted by Mohonta et al. [8] introduced a deep learning 2D-CNN model combined with wavelet transform for arrhythmia classification, achieving an impressive accuracy of 99.65% In their

ISSN: 2632-2714

research, Eltrass et al. [9] presented a hybrid approach that integrates deep neural networks, ECG features, and HRV measures to improve the accuracy of ECG classification. The proposed system surpasses existing methods with remarkable results, achieving an accuracy of 98.75%. This hybrid approach holds promise for real-time clinical implementation, potentially assisting cardiologists in ECG diagnosis. Losada et al. [10] used the k-Nearest Neighbor algorithm on 9000 ECG signals from the PhysioNet database, demonstrating high accuracy in normal signal classification but challenges with arrhythmias due to data imbalance. A study proposes an ECG identification method leveraging wavelet transform and probabilistic neural networks optimized by the whale optimization algorithm (WOA-PNN). This method detects Q, R, and S waves through wavelet transform and P, T waves via local windowed wavelet transform, significantly reducing ECG data dimensions. By integrating the probabilistic neural network and employing the mean impact value algorithm, less influential characteristic values are eliminated, simplifying the model. The WOAPNN approach intelligently optimizes hyperparameters, achieving high identification accuracy rates of 96.97% for a single ECG cycle and 99.43% for three cycles across the ECG-ID, MIT-BIH Normal Sinus Rhythm, and MIT-BIH Arrhythmia databases [11]. In 2022, Hammad et al. [12] have shown that multimodal approaches can significantly improve classification accuracy and efficiency in detecting arrhythmias compared to single models. Deriche et al. [13] proposed a study employing 13 ECG geometric features, based on the Pan-Tompkins QRS model, to classify five abnormal heartbeat types using the MIT-BIH arrhythmia database. The method achieves over 92% accuracy. Different features optimally identify various heartbeat abnormalities. Haleem et al. [14] proposed a method for the automatic detection of CVD via ECGs that rely on rule-based diagnosis models, which are inefficient and require significant analysis. In this paper, a two-stage multiclass algorithm is proposed, achieving 100% accuracy for congestive heart failure, 97.9% for arrhythmia, and 100% for predicting sudden cardiac deaths, surpassing state-of-the-art algorithms. The primary goal of this research is to enhance the accuracy of cardiac arrhythmia classification, contributing to the development of more effective diagnostic tools. Provide a comprehensive overview of the methodology and present the results of the experiments, which demonstrate the efficacy of the approach. Moreover, the development of such automated systems could have far-reaching implications beyond individual patient care. They could potentially streamline workflows in healthcare settings, reduce the burden on healthcare professionals, and contribute to more sustainable and efficient healthcare systems. The remainder of this paper will detail the methodology, present the findings, and discuss their implications for both clinical practice and future research.

The remainder of this paper is structured as follows:

In Section 2, present the materials and methodology, encompassing the ECG dataset, classifiers used, and the evaluation metrics. Moving on to Section 3, delve into the proposed methods, including a detailed explanation of feature extraction, classification and optimization. The subsequent Section 4 outlines the experimental setup, while Section 5 showcases the experimental results, encompassing accuracy scores, and confusion metrics and these findings are compared with related work. Finally, in Section 6, we conclude the paper by summarizing key points and suggesting potential directions for future research.

2 Material and Methods

2.1 Dataset

This paper utilizes the ECG signal dataset, that consists of Cardiac arrhythmia (ARR), Congestive heart failure (CHF), and Normal sinus rhythm (NSR) signals. The dataset comprises 162 ECG recordings obtained from Physionet databases: MIT-BIH arrhythmia database (containing 96 ARR recordings), BIDMC congestive heart failure database (containing 36 CHF recordings), and MIT-BIH normal sinus rhythm database (containing 30 NSR recordings) [15]. The data matrix is structured as a 162 *65536 array, representing a total of 162 ECG signals, each with 65536 samples. Each signal is labeled to indicate its type, enabling identification of the ECG signal category. The database is organized such that rows 1 to 96 correspond to ARR signals, rows 97 to 126 represent CHF signals, and rows 127 to 162 contain NSR signals. All ECG signals are resampled to a fixed sampling frequency of 128 Hz and normalized to remove any offset effect. Figure 1 illustrates a sample ECG signal.

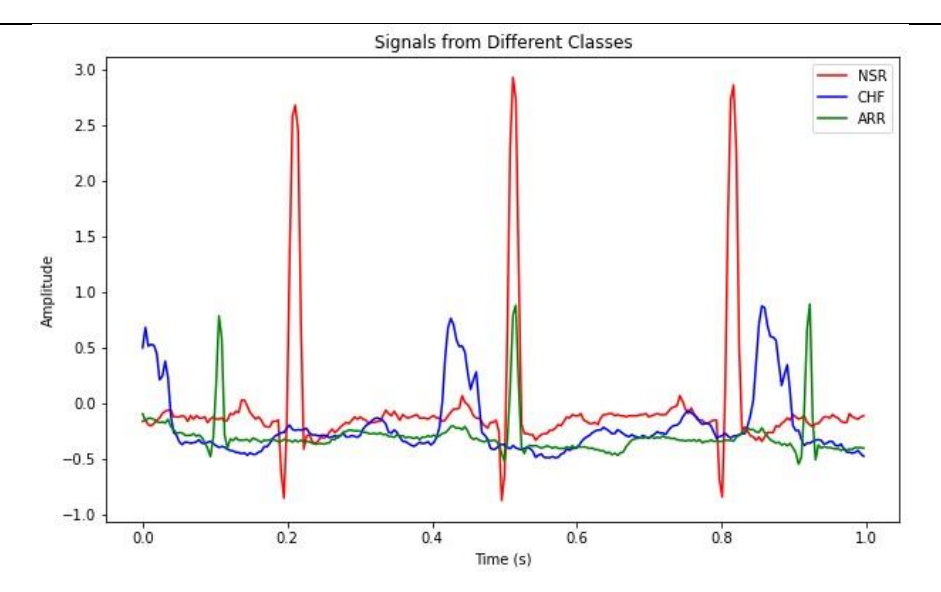


Fig. 1: Sample of ECG signals

The database is first processed at the record level. Each record, which consists of 65536 samples, is divided into smaller signals of length 1000 samples. This partitioning strategy aims to increase the size of the database. Additionally, to achieve a balanced dataset, 30 recordings of each type (ARR, CHF, and NSR) are selected. Consequently, the final dataset comprises 500 ECG signals from each category, with each signal having a length of 1000 samples.

2.2 Classifiers

Several classifiers are trained and evaluated using the input dataset. The classifiers employed in this research included the Random Forest (RF), XGBoost (XGB), Gradient Boosting (GB), Support Vector Machine (SVM), K-Nearest Neighbors (KNN), and Gaussian Naive Bayes (GNB). The training process involved fitting each classifier to the input features and their corresponding target labels. The input dataset, consisting of the features and target labels, is divided into training and testing sets. The training set is used to train the classifiers, allowing them to learn the underlying patterns and relationships in the data. After training, the classifiers are used to make predictions on the testing set.

2.3 Evaluation Standards

The effectiveness of the neural-based model system is assessed using the following metrics: accuracy, specificity, precision, sensitivity or recall, f1-score, and confusion matrix. A brief discussion of these Metrics is given below. Accuracy is the percentage of correctly categorized data instances overall data instances.

Accuracy =
$$\frac{TP + TN}{TP + FN + TN + FP}$$
 (1)

Specificity indicates the percentage of true negatives that the model accurately detects. A model with high specificity will accurately identify most of the negative outcomes, whereas one with low specificity may incorrectly classify many negative results as positive.

Specificity =
$$\frac{TN}{TN + FP}$$
 (2)

Precision indicates what percentage of identifications are actually correct.

$$Precision = \frac{TP}{(TP + FP)}$$
 (3)

Recall indicates the percentage of actual positives that are detected correctly.

Sensitivity or Recall
$$=\frac{TP}{TP + FN}$$
 (4)

score is computed by calculating the harmonic mean of two Metrics (Precision and recall). It is used to compare the performance of two classifiers.

F1 score =
$$\frac{2 \times (Precision \times Recall)}{Precision + Recall}$$
 (5)

Here, TP stands for "True Positive," FP for "False Positive," TN for "True Negative," and FN for "False Negative."

3 Proposed Method

The objective of this study is to design an automated classification system using ECG signals to accurately identify three different cardiac conditions: NSR, ARR,

and CHF. The basic block diagram illustrating the

proposed method is depicted in Figure 2.

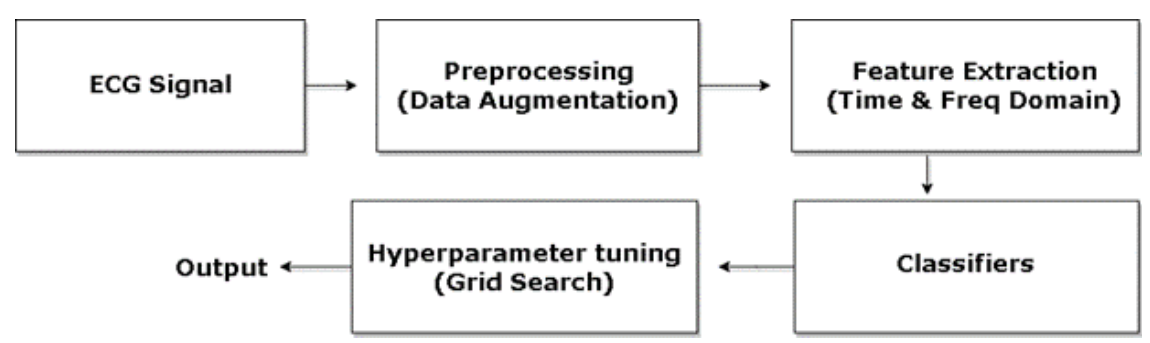


Fig. 2: Block Diagram of Proposed Method

In this experiment, taken a dataset X containing N ECG signals, each represented as a vector of M features: $X = \{x_1, x_2, ..., x_N\}$, where $x_i = [x_{i1}, x_{i2}, ..., x_N]$ x_{iM}] for i = 1, 2, ..., N. To enhance model robustness, data augmentation techniques are applied, including time-shifting and flipping the signals. Augmented data includes the original signal, a flipped version ($\mathbf{x}_{\text{flipped}}$), and a time-shifted version ($\mathbf{x}_{\text{time-shifted}}$). Feature extraction encompasses the analysis of both timedomain and frequency- domain features from each ECG signal. Time domain features include the mean $(mean(\mathbf{x}_i))$ and standard deviation $(std(\mathbf{x}_i))$. Frequency domain features are obtained using the Wavelet Packet Transform (WPT) at level 3 and include the energy of selected wavelet coefficients: E_{aad} , E_{add} , E_{dad} , and E_{ddd} as shown in fig 5. This study examined eight distinct features, which are subsequently subjected to various classification models. further, employed Grid Search to fine-tune the hyperparameters of each classifier for optimal performance. The algorithm of the proposed model is illustrated in algo. 1.

Algorithm 1: Proposed Method for ECG Signal Classification

Data: Dataset X with N ECG signals, each represented as \mathbf{x}_i with M features

Result: Classification of ECG signals using various classifiers **Input:** Extracted features from time and frequency domains **Output:** Predicted disease for ECG signal

- **1** Step 1: Database Initialization and Signal Segmentation
- **2** Load and initialize the ECG signal dataset: $X = \{x_1, x_2, \dots, x_N\}$, where each

$$x_i = [x_{i1}, x_{i2}, \dots, x_{iM}]$$
 for $i = 1, 2, \dots, N$

3 Step 2: Generate augmented datasets that include the original signal, a flipped version ($x_{flipped}$), and a

time-shifted version ($x_{time-shifted}$)

- **4** Step 3: Feature Extraction
- **5** Step 3.1: Extract time domain features for each ECG record
- 6 Mean(\mathbf{x}_i) and Std(\mathbf{x}_i)
- 7 Step 3.2: Apply Wavelet Packet Transform (WPT) with Sym4 wavelet to decompose the ECG signals at level 3
- **8** Step 3.3: Select Appropriate Bands (AAD, ADD, DAD, DDD)
- **9** Step 3.4: Calculate the energy of each selected frequency band
- **10** Step 3.5: Compute the Power Spectral Density (PSD) and Spectral Centroid (SC) from the selected energy bands
- 11 Step 4: Train classifiers (RF, XGB, SVM, GNB, KNN) using the extracted features: Mean, Std, AAD, ADD, DAD, DDD, PSD, and SC
- **12** Step 5: Apply Grid Search for Hyperparameter Optimization and Select the best hyperparameters based on cross-validation performance
- **13** Step 6: Generate predicted outputs

3.1 Data Augmentation

Two augmentation techniques have been meticulously implemented in this study: signal flipping and time—shifting. Despite the abundance of ECG data available for the classification task, these augmentation strategies offer several compelling advantages. They play a pivotal role in bolstering the model's robustness by exposing it to an expanded spectrum of data variations. This significance arises from the fact that, even within a single category of ECG signals, inherent variations persist. Augmentation augments this inherent variability, affording the model

the capacity to generalize effectively across novel instances and exhibit enhanced performance in realworld scenarios. Furthermore, the application of augmentation techniques fosters superior generalization capabilities that transcend the confines of specific instances within the dataset. By simulating divergent recording conditions, electrode placements, and signal quality variances, augmentation equips the model with the acumen to discern more resilient and broadly applicable features. In addition to its generalization benefits, augmentation acts as a form of regularization, a vital safeguard against overfitting. It promotes the model's capacity to generalize proficiently, even when confronted with extensive datasets. Therefore, even with sufficient data, augmentation techniques remain valuable for improving the performance and reliability of ECG signal classification models. This augmentation technique can potentially improve the model's ability to detect and classify abnormal arrhythmias and congestive heart failure ECG signals.

Table 1: Model Performance with and without Data Augmentation

Classifier	Accuracy (Without Augmentation)	Accuracy (With Augmentation)
Random Forest	92.33%	95.00%
XGBoost	92.00%	99.58%
SVM	41.67%	37.5%
KNN	52.00%	67.00%

Data augmentation significantly enhances the performance of the ECG signal classification model. As shown in Table 1, the accuracy of Random Forest increased from 92.33% to 95.00%, XGBoost from 92.00% to 99.58%, and KNN from 52.00% to 67.00%. This demonstrates that augmentation techniques improve model robustness and accuracy, even when the original dataset is sufficient.

3.1.1 Flipping

Flipping is a data augmentation technique that involves inverting the polarity of the signal. Flipping the signal can make the classification model more robust to changes in signal orientation. ECG signals can vary in orientation due to factors electrodeplacement, patientpositioning, or recordingartifacts. By augmenting the dataset with flipped signals, the model can learn to recognize patterns regardless of the signal's original orientation. Figure 3 illustrates a comparison between the original signal and its corresponding flipped signal. Given an input signal S, the flipped signal S flipped is obtained by multiplying each sample in S by -1:

$$S_{flipped} = -1 \cdot S \qquad (6)$$

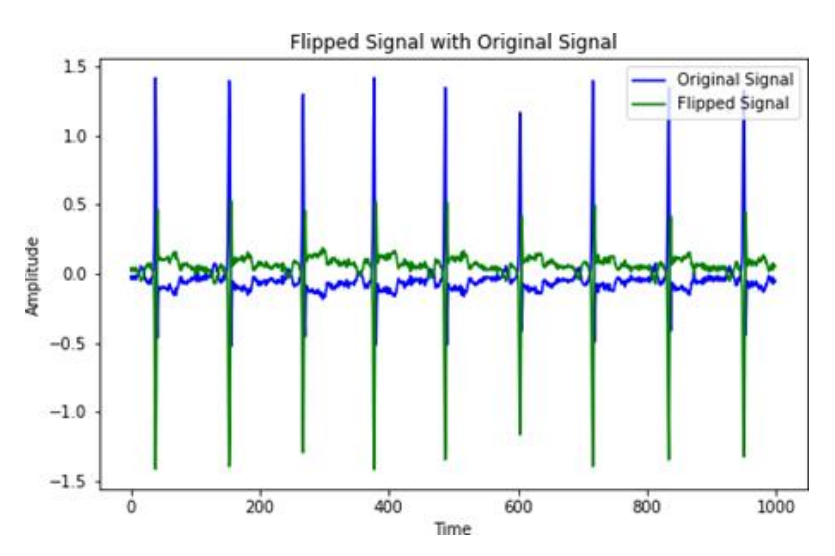


Fig. 3: Flipped Signal with Original Signal

3.1.2 Time Shifting

Figure 4 displays a comparison between the original signal and the time-shifted signal. Time-shifting is a data augmentation technique that involves shifting the signal in the time domain by a certain number of units.

In this research work, a time shift of 5 units is used. The time-shifted signal S shifted can be obtained as displayed in the equation 7. Given an input signal S, the time-shifted signal (S shifted) is obtained by circularly shifting the samples in S by a shift amount k:

$$S_{shifted[i]} = S[(i+k)modN] \tag{7}$$

where N is the length of the signal S.

3.2 Detailed Architecture of the Proposed Model for Feature Extraction

Features are extracted from ECG signals in both the time domain and the frequency domain using the WPT. Figure 5 illustrates the detailed architecture of the proposed model offering insights into the methodology behind the process of feature extraction.

3.2.1 Time Domain Features

This process aimed to capture important statistical and spectral characteristics of the signals. In the time domain, the mean (μ) and standard deviation (σ) of the signal are computed. These statistical measures provide basic information about the signal's central tendency and variability. By calculating these features, obtain information about the average amplitude and the variability of the ECG signal. These measures can help

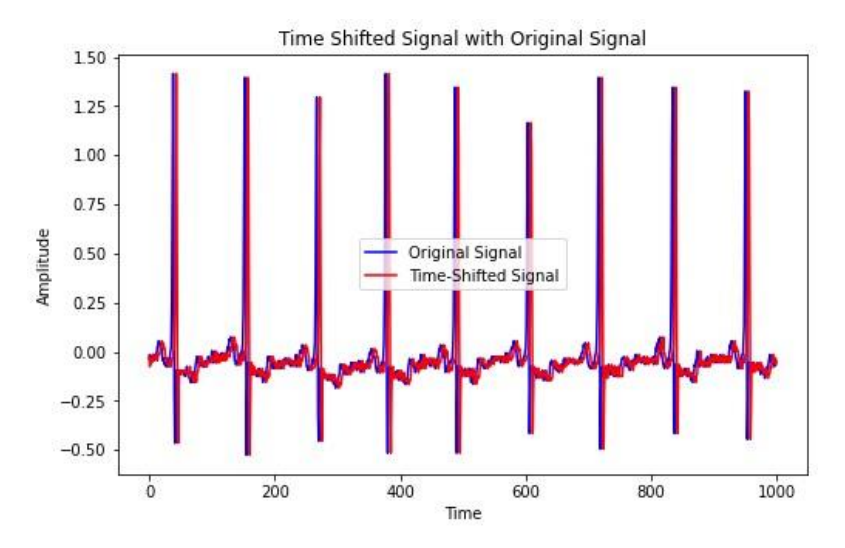


Fig. 4: Time Shifted with Original Signal

differentiate between normal and abnormal patterns in the ECG. NSR, ARR, and CHF exhibit distinct patterns in the ECG signals. Mean and standard deviation can highlight differences in signal morphology among these rhythm types. The standard deviation provides an indication of how much the signal values deviate from the mean. In the context of ECG analysis, CHF can lead to increased variability in the signal due to irregular heart contractions. Considering the standard deviation can capture this increased variability, potentially aiding in the identification of congestive heart failure. Mean and standard deviation can serve as informative features for classification algorithms. By extracting these features and combining them with other relevant features, can construct a feature vector that characterizes different ECG rhythm types.

 Mean (µ): Calculated as the average value of the signal.

$$\mu = \frac{1}{N} \sum_{i=1}^{N} x_i$$
 (8)

Here, $\boldsymbol{\mu}$ represents the mean value of the signal. N is the total number of samples

in the signal. xi represents the i^{th} sample of the signal.

 Standard Deviation (σ): Measured as the square root of the variance of the signal.

$$\sigma = \sqrt{\frac{1}{N-1} \sum_{i=1}^{N} (x_i - \mu)^2}$$
 (9)

Here, σ represents the standard deviation of the signal. N is the total number of samples in the signal. xi represents the i-th sample of the signal. μ represents the mean value of the signal.

104

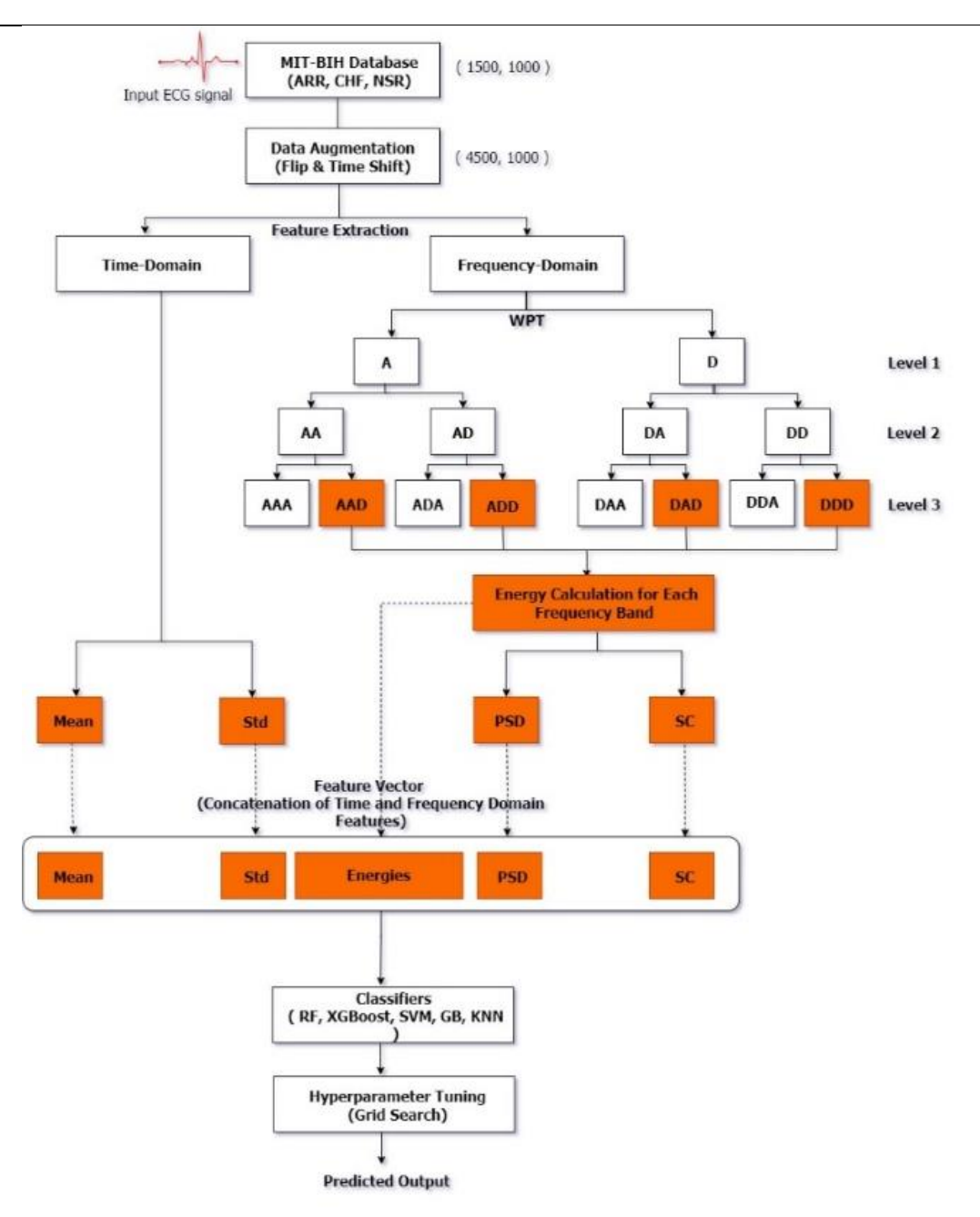


Fig. 5: Detailed Architecture of the Proposed Method

3.2.2 Frequency Domain Features Extraction using Wavelet Packet Transform

In the feature extraction process, the WPT is utilized to analyze the signal, employing the 'sym4' wavelet, which represents the fourth-order symlet wavelet—a symmetric extension of the Daubechies wavelet. WPT is an extension of the Discrete Wavelet Transform (DWT) that offers a more detailed decomposition of the signal. In the DWT, subsequent levels of the transform operate on the outputs of the Lowpass (Scaling) filter, which may not provide a complete analysis of all frequency components. In contrast, the WPT enables simultaneous processing of the results

obtained from both the Lowpass (Scaling) filter and the Highpass (Wavelet) filter at each level. The key difference is that in the undecimated discrete wavelet transform, the outputs are not downsampled. This means that the full frequency content of the signal is preserved at each level of the transform, giving a more complete analysis of the signal. For a one-dimensional signal x[n], the WPT can be expressed as:

$$WPT_{j}[n] = \sum_{k} x[k] \cdot \psi_{j,k}[n] \qquad (10)$$

Where, $WPT_j[n]$ represents a WPT coefficient at a particular node. x[k] is the input signal and $\psi_{j,k}[n]$ is the wavelet function with scale j and translation k.

ISSN: 2632-2714

Table 2: Comparative Analysis of Different Wavelets

Classifier	Accuracy	Best Parameters
RF	95.00%	Max Depth: 20, Min
		Samples Split: 2,
		Estimators: 50
XGBoost	99.58%	Learning Rate: 0.1,
		Max Depth: 7,
		Estimators: 200
SVM	37.50%	C: 1, Kernel: Linear
KNN	67.00%	Neighbors: 3, Metric:
		Minkowski (P=1),
		Weights: Distance
GNB	55.20%	Var Smoothing: 1e-9
RF	97.11%	Max Depth: None,
		Min Samples Split: 2,
		Estimators: 10
XGBoost	90.67%	Learning Rate: 0.1,
		Max Depth: 3,
		Estimators: 50
SVM	79.22%	C: 10, Gamma: Auto
KNN	70.22%	Neighbors: 3
RF	95.22%	Max Depth: None,
		Min Samples Split: 2,
		Estimators: 10
XGBoost	89.00%	Learning Rate: 0.1,
		Max Depth: 3,
		Estimators: 50
SVM	78.00%	C: 10, Gamma: Auto
KNN	69.56%	Neighbors: 3
RF	95.56%	Max Depth: None,
		Min Samples Split: 2,
		Estimators: 10
XGBoost	88.22%	Learning Rate: 0.1,
		Max Depth: 3,
		Estimators: 50
SVM	80.22%	C: 10, Gamma: Auto
KNN	70.67%	Neighbors: 3
	RF XGBoost SVM KNN GNB RF XGBoost SVM KNN RF XGBoost SVM KNN RF XGBoost	RF 95.00% XGBoost 99.58% SVM 37.50% KNN 67.00% GNB 55.20% RF 97.11% XGBoost 90.67% SVM 79.22% KNN 70.22% XGBoost 89.00% SVM 78.00% KNN 69.56% RF 95.56% XGBoost 88.22% SVM 80.22%

In table 2, results demonstrated that the 'sym4' wavelet provided the highest accuracy with the XGBoost classifier, achieving an impressive accuracy of 99.58%, surpassing other wavelets in performance metrics. The comparative results for each classifier and their optimal parameters obtained through grid search optimization are summarized in the above table 2. This comparative analysis validates the selection of the 'sym4' wavelet for the proposed ECG signal classification methodology. Furthermore, WPT offers a notably versatile approach to signal analysis, especially when the objective is to concentrate on distinct frequency bands or individual components within the signal. This technique enables researchers and analysts to discern and examine specific aspects of a signal with a high degree of precision and selectivity, making it a valuable tool in the realm of signal processing and analysis. In this work, one-dimensional ECG signal x[n] decomposes using WPT with the Symlet-4 wavelet at level 3. Here's how the decomposition proceeds:

Level 1 Decomposition (j = 1)

At the first level, the ECG signal is decomposed into approximation and detail coefficients using the Sym4 wavelet. Figure 6 displays the ECG signal graph at level 1 (A & D coefficients) with the original signal. The approximation coefficients at this level represent the low-frequency components of the ECG signal, and the detail coefficients capture high-frequency details. The decomposition is given by:

$$WPT_1[n] = \sum_{k} x[k] \cdot \psi_{1,k}[n]$$
 (11)

Here, $\psi_{1,k}[n]$ represents the Sym4 wavelet function at level 1.

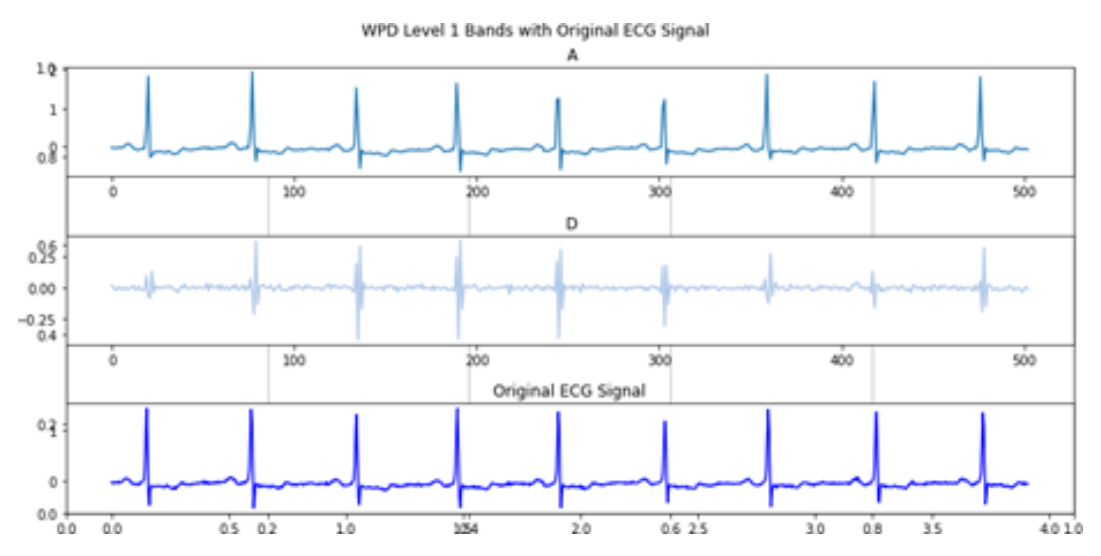


Fig. 6: WPD level 1 bands with original ECG signal

ISSN: 2632-2714

Level 2 Decomposition (j = 2)

At the second level, both the approximation and detail coefficients from level 1 are further decomposed into their own approximation and detail coefficients. Figure 7 displays the ECG signal decomposition at level 2 with the original signal. This results in a more detailed representation of the ECG signal, capturing both low and high-frequency components. The decomposition equations are as follows:

$$WPT_2^A[n] = \sum_k WPT_1^A[k] \cdot \psi_{2,k}[n]$$
 (12)

$$WPT_2^D[n] = \sum_{k} WPT_1^D[k] \cdot \psi_{2,k}[n]$$
 (13)

Here, $\psi_{2,k}[n]$ represents the Sym4 wavelet function at level 2. $WPT^A[k]$ and $WPT^D[k]$ are the approximation and detail coefficients obtained at level 1. Equ. 12 and Equ. 13 are employed in the computation of approximation coefficients (AA and AD) and detailed coefficients (DA and DD) respectively.

Level 3 Decomposition (j = 3)

At the third level, the process continues, with both the approximation and detail coefficients from level 2 undergoing further decomposition. Figure 8 displays the ECG signal decomposition at level 3 with the original signal. The equations for the third-level decomposition are as follows:

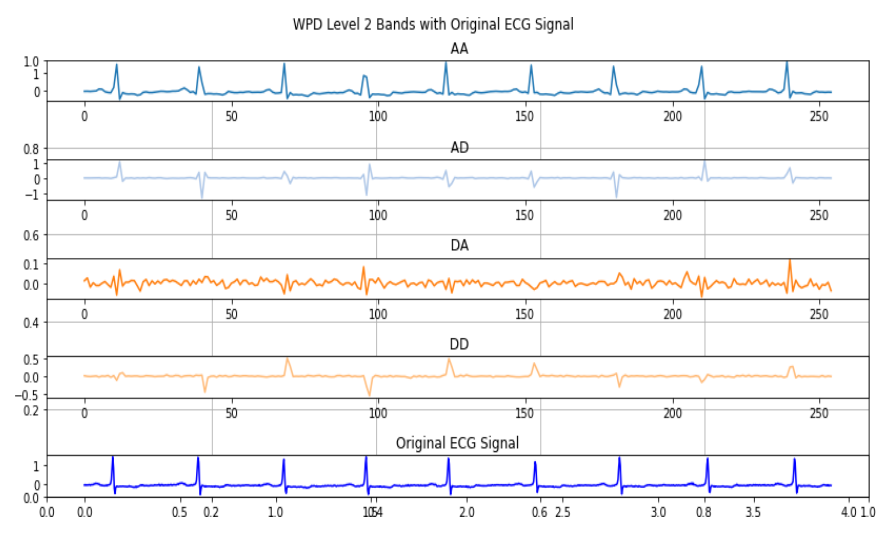


Fig. 7: WPD level 2 bands with original ECG signal

$$WPT_{2}^{A}[n] = \sum\nolimits_{k} WPT_{1}^{A}\left[k\right].\psi_{2,k}[n] \tag{14}$$

$$WPT_3^D[n] = \sum_k WPT_2^D[k] \cdot \psi_{3,k}[n]$$
 (15)

Here, $\psi_{3,k}[n]$ represents the Sym4 wavelet function

at level 3. $WPT^A[k]$ and $WPT^D[k]$ are the approximation and detail coefficients obtained at level 2. Equ. 14 and Equ. 15 are employed in the computation of approximation coefficients (AAA, AAD, ADA, and ADD) and detailed coefficients (DAA, DAD, DDA, and DDD) respectively.

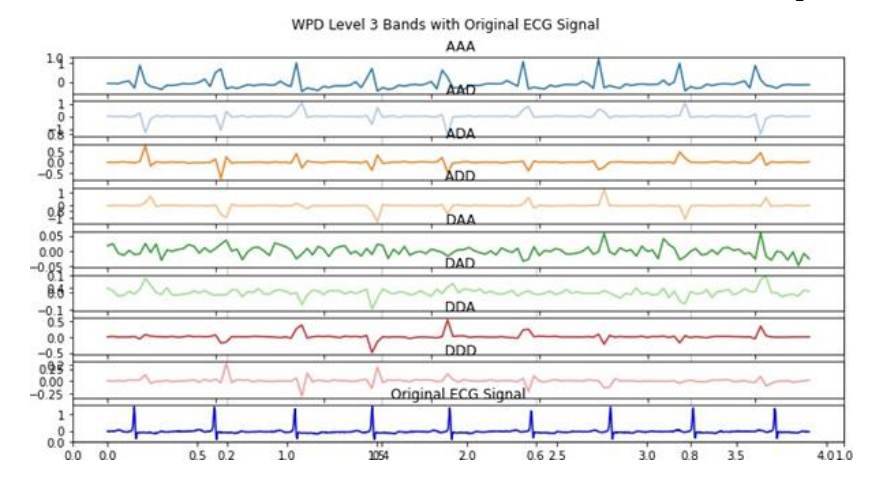


Fig. 8: WPD level 3 bands with original ECG signal

that

By performing this three-level decomposition using the Sym4 wavelet, obtain a detailed epresentation of the original one-dimensional ECG

captures

different frequency

components at various levels of detail. This multiresolution analysis is valuable for tasks such as feature extraction in ECG data. Figure 9 depicts a plot of all the bands at level 3 alongside the original signal.

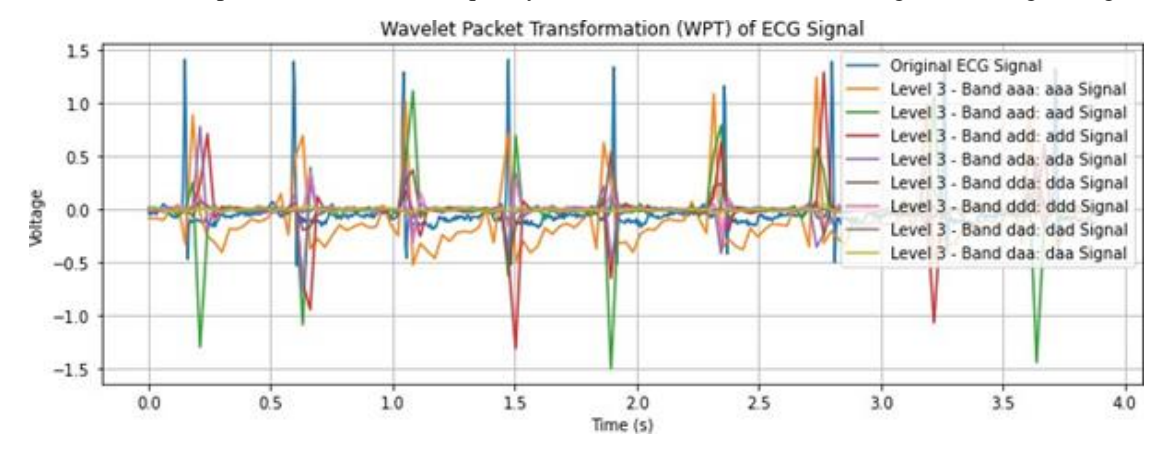


Fig. 9: WPD level 3 bands with original ECG signal

Selection of Bands at Level 3 in WPT

In the context of WPT, at level 3, there are a total of eight available bands for decomposition. These bands represent different combinations of approximation (A) and detail (D) coefficients, each capturing specific information about the signal. The eight bands at level 3 are AAA, AAD ADA, ADD, DAA, DAD, DDA, and DDD, where each letter represents whether the coefficient is an approximation (A) or a detail (D) coefficient.

For a particular signal analysis, it may be necessary to focus on specific frequency components or details within the signal. In this scenario, we have selected four bands out of the available eight for further analysis. The selected bands are as follows:

1. AAD (Approximation-Approximation- Detail):
AAD combines two levels of smoothed, lower-frequency information (AA) with the detailed high-frequency information specific to the third level.
This sub-band is capturing characteristics related to the intermediate frequency range in a signal, potentially revealing details about the morphology of ECG waveforms and different heart conditions.
AAD band plot displayed in Figure 10

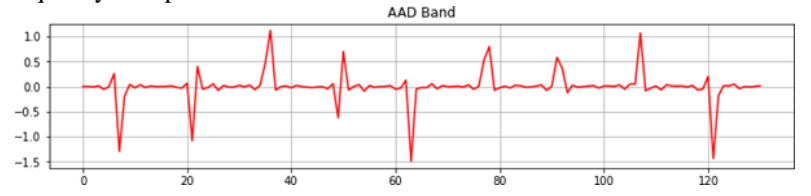


Fig. 10: AAD plot

 ADD (Approximation-Detail- Detail): It provides insights into both smoothed and highly localized changes within the signal, offering a comprehensive view of the signal's frequency components. ADD is valuable for analyzing various features, making it useful for applications like ECG analysis and the detection of cardiac conditions. Figure 11 illustrates the ADD plot.

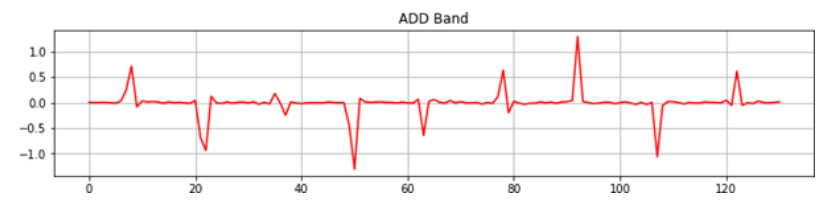


Fig. 11: ADD plot

3. **DAD** (**Detail-Approximation- Detail**): DAD band highlights high-frequency details while still preserving

essential approximation components.DAD band plot displayed in Figure 12

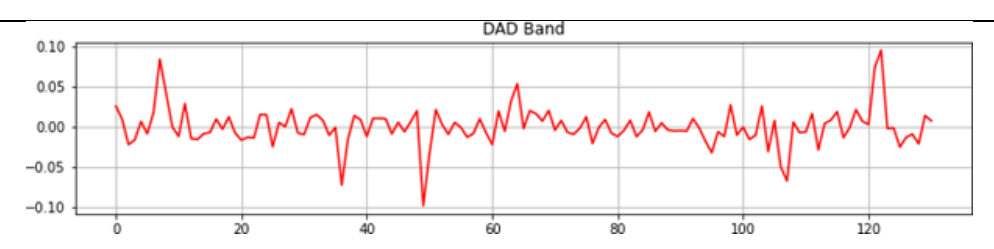


Fig. 12: DAD plot

4. **DDD** (**Detail-Detail**): This band is selected to provide a comprehensive analysis, capturing detailed high-frequency information without approximation. This sub-band is sensitive to fast and localized changes

within the signal, making it invaluable for detecting specific cardiac events, arrhythmias, and other irregularities in the ECG waveform. Figure 13 displayed a DDD plot.

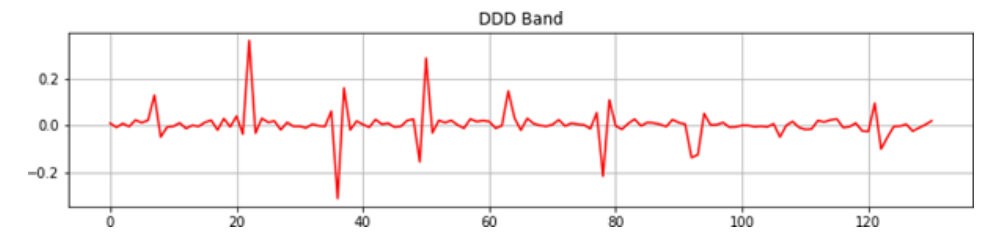


Fig. 13: DDD plot

The choice of these specific bands allows for a more targeted analysis of the signal, tailored to the requirements of the task at hand. The selection of bands in WPT provides the flexibility to focus on the aspects of the signal that are most relevant to analysis.

3.2.3 Energies, Power Spectral Density (PSD) and Spectral Centroid (SC) Calculation

By the meticulous selection of specific nodes during wavelet packet decomposition(WPD), along with the subsequent computation of their energy values (represented as the sum of squares of the coefficients), significant frequency components and their corresponding contributions to the signal's energy are discerned. These calculated energy values are then leveraged to derive essential spectral features, including *PSD* and *Spectral Centroid*. These spectral features provide valuable insights into the frequency distribution within the signal, enriching the understanding and analysis. The energy is calculated as follows.

$$Energy = \sum_{i=1}^{N} c_i^2 \qquad (16)$$

Here, 'energy' represents the energy of a selected node from the WPD. N is the total number of coefficients in the selected node. c_i represents the i^{th} coefficient of the selected node.

PSD: The PSD is derived from the energies of the selected nodes. By examining the PSD, which represents the power distribution across different

frequency bands, it can identify the dominant frequencies and their relative strengths. This information helps in understanding the underlying mechanisms of cardiac disorders.

$$PSD = \frac{1}{N} \sum_{i=1}^{N} \text{Energy}_{i}$$
 (17)

where 'PSD' represents the PSD, N is the total number of selected nodes, and energy i represents the energy value of the ith selected node.

SC: The SC is computed as the weighted average of the energies, indicating the

distribution of spectral energy.

$$SC = \frac{\sum_{i=1}^{N} i \cdot Energy_i}{\sum_{i=1}^{N} Energy_i}$$
 (18)

The SC represents the weighted average of the energy values of N selected nodes.

Let N be the total number of selected nodes, i be the index of the selected node, and $energy_i$ be the energy value of the ith selected node. Then, the SC can be calculated as above Equ. 18 changes in the PSD and SC can provide quantitative measures of alterations in the frequency characteristics of ECG signals. These changes may indicate the progression or severity of cardiac conditions, including CHF. Tracking these measures over time can assist in monitoring the

effectiveness of treatments or interventions. The process commences with the extraction of informative features from the input ECG signals. Both time and frequency domain analyses are deployed to encapsulate pertinent characteristics. In the time domain, statistical attributes, specifically the mean and standard deviation, furnish insights into the overall signal morphology. Meanwhile, in the frequency domain, the 'sym4' wavelet is employed for WPT, and energy values are derived from selectively chosen nodes at level 3. These energy values provide valuable insights into the spectral attributes of the ECG signals. Each classifier acquires the distinctive attributes associated with

ARR, CHF, and NSR ECG signals.

3.2.4 Feature Importance

A total of eight features are derived from both the time and frequency domains. Within the time domain, we calculate the mean (μ) and standard deviation (σ) of the signal. In the frequency domain, assess the energies within four specific bands through the WPT, as well as evaluate the PSD and the SC. The visual representations of these extracted features, depicted in Figure 14, offer a visual means of understanding their distribution and patterns.

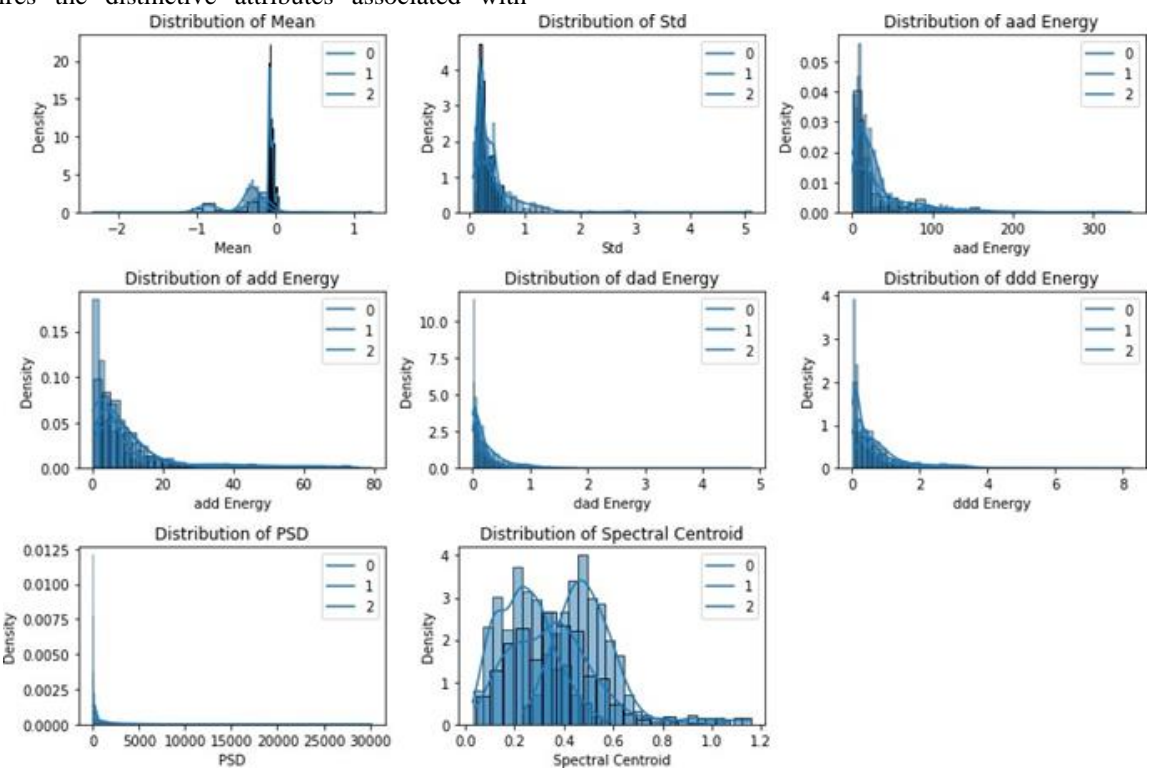


Fig. 14: Features Visualization

The Displayed Figure 14 comprises a 3 x 3 grid of subplots, each displaying a feature's distribution extracted from signals. The x-axis represents feature values, while the y-axis depicts occurrence density via Kernel Density Estimation (KDE). Histogram shapes reveal value distribution, with taller bars indicating higher density. KDE curves offer insights into underlying probability density functions. The analysis yields insights such as unimodal or bimodal distributions, spread, skewness, and overall shape, aiding anomaly detection, feature selection, and data insights. The graph represents the distribution of different features extracted from the dataset. Each subplot in the graph shows the histogram of a specific feature, and the histograms are differentiated by the target labels (0, 1, 2). In the graph, each subplot corresponds to one of these features. The x-axis represents the value range of the respective feature, and the y-axis represents the density of occurrences within that value range. The legend at the top right corner of the graph represents the target labels. In this case, the labels 0, 1, and 2 represent different classes or categories of the data. These labels could correspond to different types of signals or patterns that are being classified or analyzed. By observing the histograms and the differentiation based on the target labels, we can gain insights into the distribution and patterns of the features across different classes. It allows us to understand how the feature values are distributed within each class and whether there are noticeable differences or similarities between the classes.

ISSN: 2632-2714

3.3 Hyperparameters Optimization

The optimization of hyperparameters is achieved through the utilization of grid search, and methodical exploration of predefined hyperparameter values to maximize their performance. This iterative process serves to finely adjust the models and capture intricate relationships within the ECG signal data. In the thorough evaluation of diverse machine learning classifiers for the classification of ECG signal classes, an investigation is conducted into the performance of RF, XGB, GB, SVM, KNN, and Gaussian Naive Bayes algorithms. Among these classifiers, XGBoost emerges as the leading model following an exhaustive hyperparameter tuning process involving grid search. Through the grid search, identified the optimal hyperparameters for the XGBoost model that led to the best results in terms of classification accuracy and performance. Specifically, achieved superior results with a learning rate of 0.1, a maximum depth of 7 for each boosting tree, and the use of 200 estimators. This combination of hyperparameters resulted in a wellgeneralized and robust model, capable of accurately distinguishing between different ECG signal classes. Table 3 presents the optimal parameters corresponding to each classifier.

4 Experimental Setup

The experimental setup involved implementing the proposed ECG signal classification method using Python and libraries such as NumPy, pandas, scikitlearn, XGB, pywt, and matplotlib. These tools are employed for data processing, manipulation, machine learning, boosting, feature extraction through Wavelet Packet Transform, and visual representation of results.

5 Experimental Results & Discussion

Based on the experimental results, indicating its ability to accurately classify ECG signals. RF and GB demonstrated exceptional performance, achieving both high specificity and accuracy, with specificity values of 97.00% and 98.15%, and accuracy values

Table 3: Optimal Hyperparameters for Proposed Model's Classifiers using Grid Search

Parameter	Value
learning rate	0.1
max depth	7
estimators	200
max depth	20
min samples	2
split	50
estimators	
cost	1
	learning rate max depth estimators max depth min samples split estimators

	parameter	linear
	kernel	
KNN	n neighbors	3
	p	1
	weights	'distance'
Gaussian	var	default (1×10^{-9})
Naive Bayes	smoothing	

of 95.00% and 96.25%, respectively, making them effective tools for cardiac condition identification. KNN and GNB also delivered notable results, with specificity and accuracy values around 83.6% and 77.61%, indicating their competence in classifying ECG signals. SVM, however, exhibited comparatively lower values for both specificity and accuracy, with values of 73.3 and 37.5%, suggesting that SVM may not be the optimal choice for this specific classification task. XGB displayed impressive specificity at 99.7% and accuracy at 99.58%, indicating its potential for detecting cardiac conditions. Figure 15 illustrates the performance Metrics for all the classifiers.

A comprehensive overview of performance metrics for various classifiers, including RF, GB, SVM, KNN, GNB and the proposed work, represented as "XGB" These metrics encompass essential evaluation criteria such as Precision, F1-Score, Sensitivity, Specificity, Accuracy, ARR, CHF, and NSR. Notably, the "XGB" classifier, representing the proposed approach, demonstrates remarkable performance across the measured metrics, with detailed insights provided in Table 4.

Using the same dataset, several additional methods are explored to optimize feature selection in classification. The first experiment utilized Particle Swarm Optimization (PSO) to enhance the accuracy of the RF, achieving an impressive 98%. In the second experiment, the Genetic Algorithm (GA) is employed for feature subset evolution and achieved 89.33% or accuracy with RF. The third experiment introduced a novel hybrid approach, PSO-GA, which synergized PSO's convergence speed and GA's adaptability, yielding a remarkable 97.78% accuracy in classifying ECG signals. Ultimately, the proposed method, incorporating the XGB classifier, attained the highest accuracy of 99.58%.

5.1 Confusion Metrics Analysis

To ensure a balanced representation, a subset of the testing set containing a fixed number of samples (80 samples per class) is selected for generating the confusion Metrics. Figure 16 displayed the confusion Metrics for different classifiers.

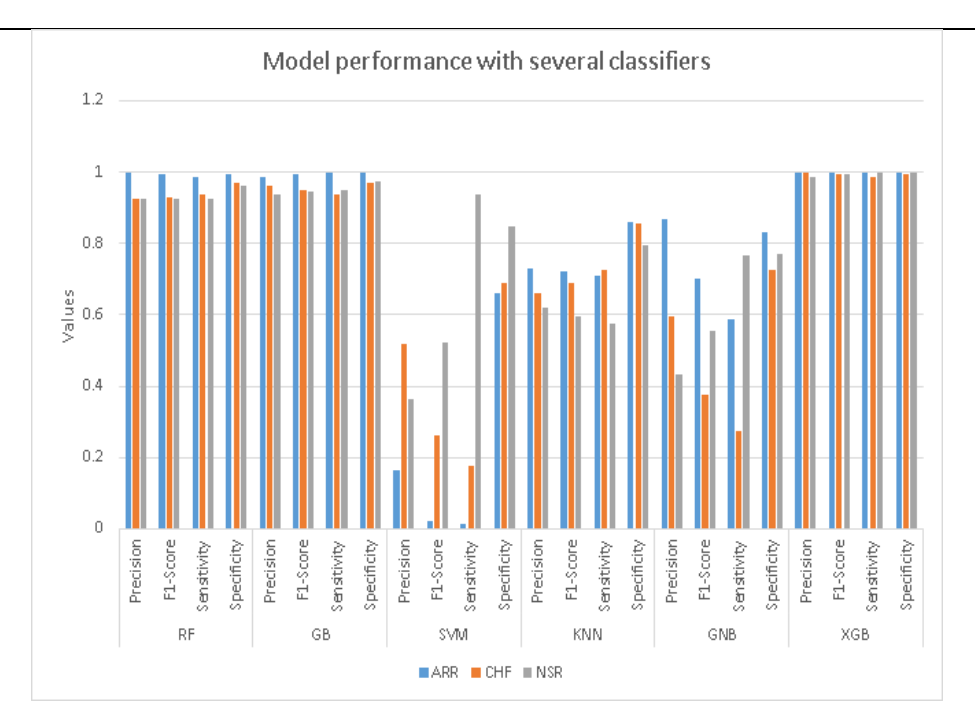


Fig. 15: performance Metrics graph

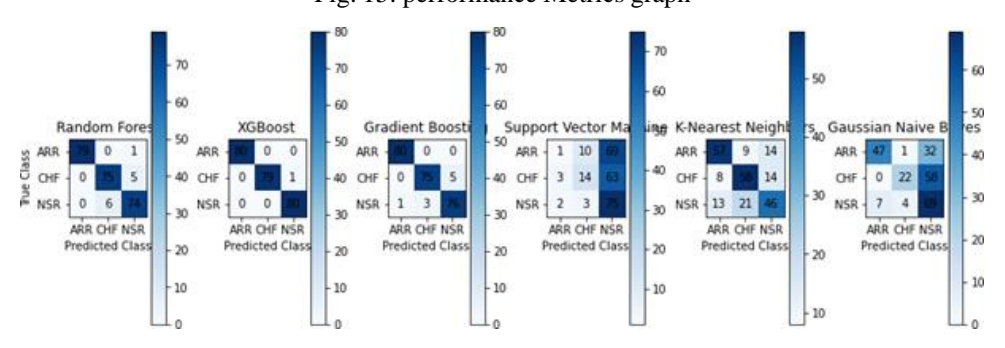


Fig. 16: Confusion Metrics

Table 5 displayed the distribution of true positive, false positive, true negative, and false negative predictions of the XGB classifier.

The confusion matrix table 5 reveals the number of true positives (TP), false positives (FP), and false negatives (FN) for each class. Notably, the classifier achieved perfect detection of Actual ARR, Actual CHF and Actual NSR cases, with TP counts of 80 for both classes. However, for Actual CHF, there is 1 FN instance, indicating cases where the model failed to

correctly classify CHF. The absence of FP in the Actual ARR and NSR categories suggests high precision in prediction. Overall, the confusion matrix highlights the strengths of the classifier in differentiating between the classes, and these models hold great promise for accurate cardiac disease diagnosis and patient care.

Table 4: Performance metrics

Classifiers	Performance	ARR	CHF	NSR	Over all	Over all
	Metrics				Specificity	Accuracy
	Precision	1	0.925	0.925		
RF	F1-Score	0.993	0.931	0.925	0.97	0.95
	Sensitivity	0.987	0.937	0.925		
	Specificity	0.993	0.968	0.962		
	Precision	0.987	0.961	0.938		
GB	F1-Score	0.993	0.949	0.944	0.9813	0.9625
	Sensitivity	1	0.937	0.95		

ISSN: 2632-2714

	Specificity	1	0.969	0.974		
	Precision	0.166	0.518	0.362		
SVM	F1-Score	0.0232	0.261	0.522	0.733	0.375
	Sensitivity	0.012	0.175	0.937		
	Specificity	0.662	0.69	0.848		
	Precision	0.73	0.659	0.621		
KNN	F1-Score	0.721	0.69	0.597	0.836	0.67
	Sensitivity	0.71	0.725	0.575		
	Specificity	0.858	0.855	0.795		
	Precision	0.87	0.594	0.433		
GNB	F1-Score	0.701	0.376	0.554	0.7761	0.552
	Sensitivity	0.587	0.275	0.766		
	Specificity	[0.831	0.727	0.769		
	Precision	1	1	0.987		
XGB	F1-Score	1	0.993	0.993	0.997	0.995
	Sensitivity	1	0.987	1		
	Specificity	1	0.993	1		

Table 5: Confusion Metrics

Classifier	XGBoost			
	Predicted ARR	Predicted CHF	Predicted NSR	
Actual ARR	TP = 80	FP = 0	FN = 0	
Actual CHF	FP = 0	TP = 79	FN = 1	
Actual NSR	FP = 0	FP = 0	TP = 80	

furthermore, the proposed model boasts high accuracy (99.58% with XGBoost), robust data augmentation using flipping and time-shifting, and optimized feature extraction via Wavelet Packet Transform (WPT) with 'sym4' wavelet. Its comprehensive evaluation with multiple classifiers demonstrates superiority over traditional and deep learning methods, with significant implications for improving diagnostic accuracy, operational efficiency, and scalability in healthcare. However, the model requires substantial computational resources, relies on a relatively small dataset, and shows lower performance with SVM. Additionally, its dependence on data augmentation and the need for further realworld validation are notable limitations.

5.2 Comparison with related work

In comparison to existing methods, proposed method stands out as it attains an impressive accuracy of 99.58% on the MIT-BIH dataset, surpassing the performance of several existing methods. Porumb et al. [16] employs a CNN and achieves an accuracy of 97.8%, while Avanzato and Beritelli [17] utilizes a 1-D CNN with five layers and reports an accuracy of 98.33%. Kaspal et al. [18] combines ECG feature extraction and CNN, reaching accuracy levels of 90.60% and 93.24% for different datasets. In contrast,

Oh et al. [19] utilizes deep learning techniques such as CNN and LSTM, yielding an accuracy of 98.10%. Huang et al. [20] applies STFT spectrogram and 2D-CNN, achieving an accuracy of 99.00%, while Singh et al. [21] relies on RNN LSTM, resulting in an accuracy of 88.1%. Orhan [22] uses a CNN and reports an accuracy of 98.97%. Kaouter et al. [23] combines CNN with Continuous Wavelet Transform (CWT), obtaining an accuracy of 93.75%, and Kumari et al. [24] utilizes CWT and SVM, reaching an accuracy of 95.92%. Proposed approach, excels in accuracy, showcasing its potential for advanced healthcare applications. Comparison of the proposed method with several existing methods are displayed in Table 6.

Table 6: Comparison of proposed work with existing

D. C.	3.6.4.1	D	D 1.
Reference	Method	Dataset	Results
[16]	CNN	MIT-BIH	97.8%
		NSR	
		BIDMB	
		CHF	
[17]	1-D CNN, 5-	MIT-BIH	98.33%
	layer	NSR	
		MIT-BIH	
		Arrhythmia	
[18]	ECG features	SCD Holter	90.60%
	extraction,	MIT-BIH	93.24%
	CNN	Arrhythmia	
[19]	Deep learning,	MIT-BIT	98.10%
	CNN and	Arrhythmia	
	LSTM		
[20]	STFT	MIT-BIH	99.00%
	spectrogram		
	2D-CNN		
[21]	RNN LSTM	MIT-BIH	88.1%

ISSN: 2632-2714

		Arrhythmia	
[22]	CNN	CHF, NSR	98.97%
[23]	CNN + CWT	NSR, CHF, ARR	93.75%
[24]	CWT + SVM	CHF, NSR	95.92%
Proposed Work	Time & freq. domain features ,WPT	МІТ-ВІН	99.58%
	Energy, PSD, SC		

6 Conclusion

This study presents a novel approach to ECG signal classification by leveraging advanced augmentation techniques and optimized feature extraction using Wavelet Packet Transform with the 'sym4' wavelet. The proposed model demonstrates exceptional performance, achieving a high accuracy of 99.58% with XGBoost. These results underscore the model's robustness and effectiveness in accurately classifying arrhythmias. The use of dual data augmentation techniques, including flipping and timeshifting, significantly enhances the model's ability to generalize to unseen data, making it more reliable in practical applications. The comprehensive evaluation with multiple classifiers further validates the superiority of the proposed method over traditional and deep learning models, highlighting its efficiency and lower computational complexity.

The high accuracy and robust performance of the model have significant managerial implications, including improved diagnostic accuracy, operational efficiency, cost savings, scalability, and the potential for real-time patient monitoring. These benefits make the proposed method a valuable tool in advancing automated cardiac disease detection and enhancing patient care.

Future research could explore the integration of this model into wearable devices and telemedicine platforms, as well as its application to larger and more diverse datasets. The potential for continuous, real-time monitoring and early intervention underscores the transformative impact this technology can have on cardiovascular healthcare.

Declaration

On behalf of all authors, the corresponding author states that there is no conflict of interest.

Ethical Approval

This article does not contain any studies which human participants or animals performed by any of the authors.

References

- [1] Manish Sharma, Ru-San Tan, and U Rajendra Acharya. Automated heartbeat classification and detection of arrhythmia using optimal orthogonal wavelet filters. *Informatics in Medicine Unlocked*, 16:100221, 2019.
- [2] Enbiao Jing, Haiyang Zhang, ZhiGang Li, Yazhi Liu, Zhanlin Ji, Ivan Ganchev, et al. Ecg heartbeat classification based on an improved resnet-18 model. *Computational and Mathematical Methods in Medicine*, 2021, 2021.
- [3] Agostino Giorgio, Maria Rizzi, and Cataldo Guaragnella. Efficient detection of ventricular late potentials on ecg signals based on wavelet denoising and svm classification. *Information*, 10(11):328, 2019.
- [4] Chandan Kumar Jha and Maheshkumar H Kolekar. Cardiac arrhythmia classification using tunable q-wavelet transform based features and support vector machine classifier. *Biomedical Signal Processing and Control*, 59:101875, 2020.
- [5] Maheswari Arumugam and Arun Kumar Sangaiah. Arrhythmia identification and classification using wavelet centered methodology in ecg signals. *Concurrency and computation: practice and experience*, 32(17):e5553, 2020.
- [6] Yunxiang Zhao, Jinyong Cheng, Ping Zhang, and Xueping Peng. Ecg classification using deep cnn improved by wavelet transform. *Computers, Materials and Continua*, 2020.
- [7] Tao Wang, Changhua Lu, Yining Sun, Mei Yang, Chun Liu, and Chunsheng Ou. Automatic ecg classification using continuous wavelet transform and convolutional neural network. *Entropy*, 23(1):119, 2021.
- [8] Shadhon Chandra Mohonta, Mohammod Abdul Motin, and Dinesh Kant Kumar. Electrocardiogram based arrhythmia classification using wavelet transform with deep learning model. *Sensing and Bio-Sensing Research*, 37:100502, 2022.
- [9] Ahmed S Eltrass, Mazhar B Tayel, and Abeer I Ammar. Automated ecg multiclass

- classification system based on combining deep learning features with hrv and ecg measures. *Neural Computing and Applications*, 34(11):8755–8775, 2022.
- [10] Diego Fernando Sendoya Losada, Julián Jos´e Soto Gómez, and Julián Andr´es Zúñiga Vela. Classification of ecg signals using machine learning techniques. *Academic Journal of Interdisciplinary Studies*, 13(3):92, May 2024.
- [11] Ning Li, Fuxing He, Wentao Ma, Ruotong Wang, Lin Jiang, and Xiaoping Zhang. The identification of ecg signals using wavelet transform and woa-pnn. *Sensors*, 22(12):4343, 2022.
- [12] Mohamed Hammad, Souham Meshoul, Piotr Dziwiński, Pawe-l P-lawiak, and Ibrahim A Elgendy. Efficient lightweight multimodel deep fusion based on ecg for arrhythmia classification. *Sensors*, 22(23):9347, 2022.
- [13] Mohamed Deriche, Saeed Aljabri, Mohammed Al-Akhras, Mohammed Siddiqui, and Naziha Deriche. An optimal set of features for multiclass heart beat abnormality classification. In 2019 16th International Multi-Conference on Systems, Signals & Devices (SSD), pages 418–422. IEEE, 2019.
- [14] Muhammad Salman Haleem, Rossana Castaldo, Silvio Marcello Pagliara, Mario Petretta, Marco Salvatore, Monica Franzese, and Leandro Pecchia. Time adaptive ecg driven cardiovascular disease detector. *Biomedical Signal Processing and Control*, 70:102968, 2021.
- [15] Ary L Goldberger, Luis AN Amaral, Leon Glass, Jeffrey M Hausdorff, Plamen Ch Ivanov, Roger G Mark, Joseph E Mietus, George B Moody, Chung-Kang Peng, and H Eugene Stanley. Physiobank, physiotoolkit, and physionet: components of a new research resource for complex physiologic signals. *circulation*, 101(23):e215–e220, 2000.
- [16] Mihaela Porumb, Ernesto Iadanza, Sebastiano Massaro, and Leandro Pecchia. A convolutional neural network approach to detect congestive heart failure. Biomedical Signal Processing and Control, 55:101597, 2020.
- [17] Roberta Avanzato and Francesco Beritelli. Automatic ecg diagnosis using convolutional neural network. *Electronics*, 9(6):951, 2020.

- [18] Rabin Kaspal, Abeer Alsadoon, PWC Prasad, Nedhal A Al-Saiyd, Tran Quoc Vinh Nguyen, and Duong Thu Hang Pham. A novel approach for early prediction of sudden cardiac death (scd) using hybrid deep learning. *Multimedia Tools and Applications*, 80:8063–8090, 2021.
- [19] Shu Lih Oh, Eddie YK Ng, Ru San Tan, and U Rajendra Acharya. Automated diagnosis of arrhythmia using combination of cnn and lstm techniques with variable length heart beats. *Computers in biology and medicine*, 102:278–287, 2018.
- [20] Jingshan Huang, Binqiang Chen, Bin Yao, and Wangpeng He. Ecg arrhythmia classification using stft-based spectrogram and convolutional neural network. *IEEE access*, 7:92871–92880, 2019.
- [21] Shraddha Singh, Saroj Kumar Pandey, Urja Pawar, and Rekh Ram Janghel. Classification of ecg arrhythmia using recurrent neural networks. *Procedia computer science*, 132:1290–1297, 2018.
- [22] Umut Orhan. Real-time chf detection from ecg signals using a novel discretization method. *Computers in biology and medicine*, 43(10):1556–1562, 2013.
- [23] Karboub Kaouter, Tabaa Mohamed, Dellagi Sofiene, Dandache Abbas, and Moutaouakkil Fouad. Full training convolutional neural network for ecg signals classification. In *AIP conference proceedings*, volume 2190. AIP Publishing, 2019.
- [24] Ch Usha Kumari, R Ankita, T Pavani, N Arun Vignesh, N Tarun Varma, Md Aqeel Manzar, and A Reethika. Heart rhythm abnormality detection and classification using machine learning technique. In 2020 4th International Conference on Trends in Electronics and Informatics (ICOEI)(48184), pages 580–584. IEEE, 2020.